THERMAL EFFECTS IN WALLS OF NUCLEAR CONTAINMENTS - ELASTIC AND INELASTIC BEHAVIOR

G. GURFINKEL,

Department of Civil Engineering,
University of Illinois, Urbana, Illinois, U.S.A.

ABSTRACT

Design of containment structures requires evaluation of the thermal effects created by the temperature differential between inside and outside faces. Numerical methods are presented which permit evaluation of thermal effects on reinforced concrete sections subjected to axial load and bending. The wall section of an actual containment is studied for thermal effects under various loading conditions using both elastic and inelastic analysis. The results are compared and interpreted using interaction diagrams.

1. INTRODUCTION

The design of secondary concrete containments for nuclear reactors, requires evaluation of the thermal effects introduced by the difference between outside and inside temperatures. The former may be as low as -20°F and the latter as high as 130°F. The temperature differential between the faces of the containment wall during operation of a nuclear power plant may be 100°F.

In a freely standing wall, a thermal differential generates neither forces nor moments on the wall but creates an axial distortion accompanied by a constant curvature along the entire length of the wall. The same thermal differential applied to a wall fully restrained by unyielding supports creates no distortions but generates restraining forces and moments which may be of considerable magnitude. The preceding are examples of extreme cases. Freely standing, unattached containments are affected only by changes in curvature and moment and not by axial distortions and load. The reason for this is as follows. In spite of the thermal differential, temperatures may be considered uniformly distributed in both the outside and inside faces of the containments, thereby justifying the assumption of uniform axial distortions of the wall. Because of this, the structural dome that forms the top of containments is subjected to uniform vertical displacements and does not exert any restraining axial action on the walls. However, continuity exists between the walls and the foundation slab at the bottom and the dome at the top. Therefore, the wall is rotationally restrained and any thermal differential will create changes in curvature and bending moments in it.

The evaluation of the bending moment, ΔM, induced in a wall of an unattached containment, by a given thermal differential, is the object herein. Two methods of analysis are used; namely, elastic and inelastic. Elastic analysis complies with the provisions of the working stress and yield strength design methods; inelastic analysis allows for a more realistic determination of thermal effects as it makes no simplifying assumptions. The results of both analyses are compared and the effects of various parameters on induced thermal moments are fully discussed. The wall section of an actual containment is used, as an illustrative example, for the determination of thermal effects under various loading conditions that may be present during the estimated life of the power plant.

2. ELASTIC ANALYSIS

2.1 Method of Solution: The wall shown in Fig. 1 is subjected to the action of a force N which is located at a distance e from the center line of the section. The force N is due to the combined action of external loading and the axial posttensioning applied to the wall. The eccentricity of N is due to the action of a bending moment M imposed by any of various loading conditions. It is assumed that both N and M have been obtained elsewhere and are given. Thermal effects are created by the difference in temperatures between T_i, the operating temperature inside the container and T_o, the outside ambient temperature. The temperature inside the wall is assumed to vary linearly between the values given for the faces. This results in a linear distribution of strains as shown in Fig. 1(c). The thermal gradient is given by $(T_i-T_o)/t$ and the curvature imposed on the section by the difference in strains is given by $\phi_T=\alpha(T_i-T_o)/t$ where α is the coefficient of expansion of concrete and t is the thickness of the wall.

The conditions of restraint of the wall determine the temperature effects. In what follows, the wall will be assumed to be free to expand or contract in the longitudinal direction; axial thermal deformations may take place freely without creating restraining forces, i.e. $\Delta N=0$. However, continuity of the wall with the foundation slab and top dome will create restraining moments ΔM that will depend on the thermal differential ΔT. The object herein is the determination of ΔM for a given wall section of an unattached containment subjected to the simultaneous action of N, M and ΔT. The following conventional assumptions are made:

1. A plane section normal to the axis of the wall before bending, remains plane after bending; strains are linearly distributed in the section.
2. The stress-strain relation for concrete is a straight line.
3. Concrete takes no tensile stresses. The section is considered cracked wherever the concrete is subjected to tensile strains.
4. The modular ratio $n=E_s/E$, where E_s and E are the modulus of elasticity of steel and concrete, respectively, is used to determine tensile stresses in the steel [1]. To determine compression stresses in the steel, the value 2n is used.
5. Time effects due to creep, changes in concrete properties with temperature, and transient distributions of temperature in the wall section, are ignored.

The initial and final strain distributions in the section are shown in Fig. 2(a). The initial distribution is given by strains ε_c in the concrete and ε_s in the tension steel due to eccentric loading alone. To obtain the final strain distribution, ε_c and ε_s are incremented by $\Delta\varepsilon_c$ and $\Delta\varepsilon_s$, respectively, due to temperature effects. The internal forces acting on the section and the final elastic stress distribution are shown in Fig. 2(b). Vertical equilibrium of internal and external forces can be expressed by the following equation:

$$\int_A f dA = N \tag{1}$$

Moment equilibrium of internal and external forces about the neutral axis yields:

$$\int_A fx dA = N(e'+a) + E\bar{I}\phi_T \tag{2}$$

where f is the stress of a given point at a distance x from the neutral axis, e' and a are the distances of the force and the neutral axis respectively, to the compression edge of the section and $E\bar{I}$ is the stiffness of the section about the centroid of the cracked section. Substituting $f=(f_c/a)x$ for f in Eqs. 1 and 2 yields

$$\frac{f_c}{a}\int_A x\,da = N \tag{3}$$

$$\frac{f_c}{a}\int_A x^2 dA = N(e'+a) + E\bar{I}\phi_T \tag{4}$$

Substituting $S=\int_A x dA$ in Eq. 3 gives $f_c/a=N/S$. Substitution of N/S for f_c/a and $I=\int_A x^2 dA$ in Eq. 4 yields

$$N\frac{I}{S} = N(e'+a) + E\bar{I}\phi_T \tag{5}$$

where I, S and $\bar{I}$ are functions of the independent variable a. Eq. 5 is used in the determination of the actual value of a for given values of N, e' and ϕ_T. Once a is found, the thermal effect $\Delta M=E\bar{I}\phi_T$ may be readily evaluated.

It seems advisable at this stage to emphasize the difference between the terms $\bar{I}$ and I and to explain the origin of the term $E\bar{I}\phi_T$. The term $\bar{I}$ is the moment of inertia of the final section about CG, its centroid, as shown in Fig. 2(a); I is the moment of inertia of the final section about the neutral axis. $\bar{I}$ has a lower limit given by I_c, the moment of inertia of the transformed cracked section subjected to pure bending moment and an upper limit given by I_u, the moment of inertia of the transformed uncracked section about its centroid. The relation $\bar{I}=I=I_c$ is true only under the action of pure bending moment, for which case the centroid of the section is at the neutral axis. For any other case, where $N>0$ and $\Delta T>0$, $I_c<\bar{I}<I_u$ and $\bar{I}<I$. It is easy to show that the additional moment due to temperature effects is given by the term $E\bar{I}\phi_t$. Because of the condition that $\Delta N=0$, increments of stresses Δf must meet the condition that $\int_A(\Delta f)dA=0$. Also, $\Delta M=\int_A(\Delta f)z dA$, where z measures the distance to the axis about which ΔM takes place. Let $\Delta f_c\neq 0$ be the increment of stress at the extreme fiber at the distance $z_c\neq 0$ from the axis of bending; then, $\Delta f=(\Delta f_c/z_c)z$. Substituting Δf in $\int_A(\Delta f)dA=0$ yields $\int_A z dA=0$. The latter is true only if the axis of bending, about which the additional moment due to temperature effects takes place, is the centroidal axis of the actual section. Substituting Δf in the expression for ΔM yields $\Delta M=\frac{(\Delta f_c)}{z_c}\int_A z^2 dA$. Actually, $\Delta f_c=(\Delta\varepsilon_c)E$ where $\Delta\varepsilon_c$ is the increase in strain in the extreme fiber, as shown in Fig. 2(a). Also, $\Delta\varepsilon_c=z_c\phi_T$ and $\int_A z^2 dA=\bar{I}$. Substituting the preceding values in the equation for ΔM yields $\Delta M=E\bar{I}\phi_T$, as used in Eq. 5.

2.2 Iteration Method: A closed form solution of Eq. 5 is not possible. Even when all unknown terms may be expressed as functions of the independent variable a, however laborious this might be, substitution in Eq. 5 leads only to a high order polynomial in a. An iterative method of solution is clearly indicated. For this purpose, Eq. 5 is transformed as follows:

$$R = N(e'+a) + E\bar{I}\phi_T - N\frac{I}{S} \qquad (6)$$

where R is a remainder. Theoretically, the solution is obtained when R=0. The variable selected for use in the iteration method is a. The lower bound of a is the value obtained when the section is subjected to bending moment only. However, there is no upper bound for a, as very large values may be obtained when the resulting eccentricity of the combined action of load and thermal effects is small.

The method of iteration is illustrated in Table 1 for a given section. The various terms of Eq. 6 for the assumed values of a are shown in Table 1. The initial values of a, used for cycles 1 and 2, were arbitrarily selected as equal to t/2 and 1.1 times the lower bound for a, respectively. Successive values of a are obtained by linear interpolation aiming at making R=0. The thermal effect is the value of $E\bar{I}\phi_T$ for the final cycle, i.e. ΔM=1335 Kip-in.

2.3 Influence of Various Parameters: The properties of the wall section used in the iteration example are listed in Table 1. The same wall section may be used for discussion of the influence of various parameters in creating thermal moments ΔM. In order to gain insight in the phenomenon, various combinations of axial load, moments and thermal gradients are considered as follows.

The influence of the simultaneous action of axial load N and moment M on ΔM can be studied by means of the parameter e/t, where e=M/N. Using a computer program developed to solve Eq. 5, results were obtained for various e/t ratios for the given section. The results are plotted in Fig. 3 for ΔT=100°F. For any given value of N, the additional moment ΔM due to the assumed thermal differential is a function of the paremeter e/t. As e/t increases, ΔM decreases. The various curves are bound by two limits: an upper one given for e/t=0, when the section is subjected only to N, and a lower one given for e/t=∞ when the section is subjected only to M. The upper limit of ΔM is given by $E\bar{I}\phi_T$ where $I=I_u$, the stiffness of the uncracked section. The lower limit of ΔM is given by $E\bar{I}\phi_T$ where $\bar{I}=I_c$, the stiffness of the cracked section. Any intermediate value of ΔM is due to the fact that the section is somewhat cracked, although the extent of cracking is less than that which occurs under pure bending moment. The dashed portion of the curves of Fig. 3 are solutions beyond the limits of the Working Stress Design Method [1].

It can be seen from Fig. 3 that, in addition to the e/t=0 curve, various other curves (at increasingly higher values of N) tend to intersect the upper bound for ΔM. This is true as long as $e/t \leq e_k/t$, where e_k is the eccentricity of the extreme kern point. Beyond $e=e_k$ it is theoretically impossible, no matter how large N becomes, to reach the upper bound for ΔM. This is true because the section, even in the absence of a thermal gradient, is already cracked and therefore its moment of inertia is less than I_u.

2.4 Example of Thermal Effects in an Actual Containment: The section used before corresponds to a preliminary design for the wall of the containment of an actual nuclear power plant. The various load combinations to which the wall section might be subjected are shown in Fig. 4. The letter symbols without subscripts are identified in the load combination table of the figure and are used to denote the various design conditions imposed on the wall section. The subscripted symbols are used to represent the final conditions including thermal effects.

Results are presented for two thermal differentials, namely $\Delta T=50°F$ and $\Delta T=100°F$. For load combinations K, M, and Q, the thermal gradients induce moments of the same direction as the existing moments. In these cases, the bending moment is always incremented. The increment, however, would have been greater in absolute value if the thermal curvature had been of different direction. The reason is the following. As shown elsewhere, ΔM is proportional to the final stiffness of the section. Any loss in section stiffness tends to reduce ΔM and any gain in section stiffness tends to increase ΔM. When the existing curvature and that due to the thermal gradient are additive, cracking of the section is increased with consequent loss of stiffness. Obviously the reverse is true when the thermal curvature subtracts from the existing curvature. This occurs for the other load combinations shown in Fig. 4, namely L, N, P, S and R. For these cases the thermal effects change the sign of the final moment and cause the location of the maximum compressive stress in the section to move to the opposite edge.

It may be noticed also that doubling the thermal differential from 50°F to 100°F does not double the thermal effects. On the contrary, it is immediately apparent that the additional thermal effects are smaller in all cases. Obviously, the reason for this is the increased cracking and loss of stiffness that takes place in the section when the curvature due to the increased thermal gradient is added.

It is possible to check at a glance whether or not thermal effects have made the various load combinations exceed design specifications. For this purpose, interaction diagrams axial load N vs. bending moment M can be used. An interaction diagram creates an actual boundary for combinations of N and M which do not exceed the design conditions. Only the bottom portions of the interaction diagrams are shown in Fig. 4; they correspond to the following methods of design: working stress, WSD, yield strength, YSD, and ultimate strength, USD. Nothing needs to be said about interaction diagrams based on WSD and USD methods, as both have been used for a number of years and information is readily available in the literature [2], [3], [4]. However, yield strength design [5], is relatively new, having been introduced for the design of containments under limiting conditions. In essence, YSD has features of both WSD and USD methods. Like in WSD, YSD assumes that concrete and steel behave elastically. However, YSD assumes a maximum elastic stress for the concrete and steel equal to $0.85f'_c$ and $0.9f_y$, respectively. Like in USD, the yield strength design method affects load combinations with appropriate load factors. Compliance with the method requires that the factored load combinations be less than the yield strength of the structure. Observation of Fig. 4 discloses the fact that all load combinations, including the effects of a 100°F thermal differential, are contained within the WSD interaction diagram. Because of the fact that some load combinations had been affected by the load factors, this

clearly shows that the wall section is somewhat conservative. Reduced interaction diagrams, for various values of ΔT, may be easily determined [6].

2.5 Approximate Solution: Several dimensionless parameters were tried to obtain a set of curves that could be used in the approximate determination of thermal moments for any given section. The result of these efforts is shown in Fig. 5 which plots the dimensionless parameters $[2/(I_u/I_c-1]\ (\Delta M/EI_c\phi_T-1)$ vs. log e/t. The curves are labeled in ascending order for values of the parameter $N/A_uE=\Delta T$ from zero to two. For a given section subjected to given values of N, M and ΔT the parameters $e/t=M/Nt$ and $N/A_uE=\Delta T$ may be readily determined. The point that represents the phenomenon may be plotted to determine the value of the parameter $[2/(I_u/I_c-1)]\ (\Delta M/EI_c\phi_T-1)$. Upon substitution of the various constants in the preceding expression the induced thermal moment ΔM can be obtained.

The application of the approximate method may be illustrated by means of an example. The case given in Table 1, for which the exact solution is available, is used for this purpose. The values of $e/t=2880/300x48=0.20$ and $N/A_uE=\Delta T=300/632x3865x5.5x10^{-6}x50=0.45$ define a point in Fig. 5 with an ordinate equal to 0.56. For the given section: $I_u=1.305x10^5$ in^4, $I_c=0.288x10^5$ in^4 and $I_u/I_c=4.52$. Also $E=3865$ ksi and $\phi_T=5.5x10^{-6}x50/48=5.72x10^{-6}$ rad./in. Substituting these values in the expression for the ordinate yields:

$$\left(\frac{2}{4.52-1}\right)\left(\frac{\Delta M}{3865x0.288x10^5x5.72x10^{-6}}-1\right)=0.56 \qquad (7)$$

from which $\Delta M=1260$ k-in. This result is only five percent below 1335 k-in., the actual value of ΔM.

3. INELASTIC ANALYSIS

3.1 Method of Solution: The actual stress distribution in the wall under the combined action of external axial load N, bending moment M and thermal differential ΔT is given in Fig. 2(c). Generally, the values of a shown in Figs. 2(b) and (c) are not equal; they are shown equal for convenience of reference to the same strain distribution given in Fig. 2(a). The assumptions made for the inelastic analysis include assumptions 1, 3 and 5 made for the elastic analysis, see Art. 2.1. The linear stress-strain relation for concrete is abandoned and, in its place, better representations of the actual relation [7], [8] are used. The stress-strain relation for the reinforcing steel is assumed general; the elastoplastic case of mild steel showing a sloping line from zero to yield stress and a horizontal line beyond, is a particular case.

The wall is assumed to behave as a beam-column. Hoop forces and moments created by shell action are ignored. For the case where biaxial compression is induced, the strength of the concrete is increased [9]. This occurs, for instance, at the base of the wall where the foundation slab restrains free thermal circumferential expansion. Tensile hoop forces create a biaxial state of stress that reduces the uniaxial strength of concrete [9]. However, tensile hoop forces are balanced at all times by circumferential posttensioning in a well designed containment. Hence, the results of this analysis, based on the uniaxial strength of concrete, may be considered conservative.

The determination of the strain distribution and curvature of a reinforced concrete section for given values of N and M has been solved [10] using Newton-Raphson's numerical method. Thus, the initial strain distribution and curvature ϕ shown in Fig. 2(a) is obtained. The induced thermal moment ΔM, due to the additional curvature ϕ_T imposed on the section, is obtained using a variation of the method given in Ref. 10. It can be assumed that, for a given section and material properties, N and M can be expressed as functions of ϕ and ε_c as follows:

$$N = N(\phi, \varepsilon_c)$$
$$N = M(\phi, \varepsilon_c) \tag{8}$$

Let ϕ_o and ε_{co} be the initial values given in Fig. 2(a), corresponding to the external load N_o and bending moment M_o. An expansion of Eq. 8 about N_o and M_o using Taylor's theorem and retaining only the linear terms yields:

$$N = N_o + \frac{\partial N}{\partial \phi}\delta\phi + \frac{\partial N}{\partial \varepsilon_c}\delta\varepsilon_c$$
$$M = M_o + \frac{\partial M}{\partial \phi}\delta\phi + \frac{\partial M}{\partial \varepsilon_c}\delta\varepsilon_c \tag{9}$$

where: $\delta\phi$ = increment of curvature necessary to produce N, M
$\delta\varepsilon_c$ = increment of top strain necessary to produce N, M
$\partial N/\partial\phi$ = rate of change of load with curvature
$\partial N/\partial\varepsilon_c$ = rate of change of load with top strain
$\partial M/\partial\phi$ = rate of change of moment with curvature
$\partial M/\partial\varepsilon_c$ = rate of change of moment with top strain

For the unattached containment $\Delta N=0$, i.e. $N=N_o$. Also $\delta\phi=\phi_T$ and $M-M_o=\Delta M$. Eq. 9 may be transformed into

$$\delta\varepsilon_c = -\frac{\partial N/\partial\phi}{\partial N/\partial\varepsilon_c}\phi_T$$
$$\Delta M = \left(\frac{\partial M}{\partial\phi} - \frac{\partial M}{\partial\varepsilon_c}\frac{\partial N/\partial\phi}{\partial N/\partial\varepsilon_c}\right)\phi_T \tag{10}$$

where the four different rates of change can be determined numerically from Eq. 8. Because of the approximation involved in Eq. 9, it is likely that the solution obtained from Eq. 10 in the initial trial is only approximate and does not meet the desired accuracy. The necessary check on the accuracy of the solution can be made using Eq. 8 with $\phi=\phi_o+\phi_T$ and $\varepsilon_c=\varepsilon_{co}+\delta\varepsilon_c$. If the resulting value of N is different from N_o, say $N-N_o=\Delta N\neq 0$, a better value of ε_c may be obtained by adding to it $\delta\varepsilon_c=\Delta N/\partial N/\partial\varepsilon_c$ as given by Eq. 9 for constant curvature. Using the new value of ε_c and $\phi_o+\phi_T$, Eq. 8 is checked again. The process is repeated until the desired accuracy is obtained.

A digital computer program based on the preceding method was used to analyze the section of Table 1, for inelastic behavior. Hognestad's stress-strain diagram [7] was adopted; the maximum stress of concrete being $0.85f'_c$ at a strain $\varepsilon_c=0.002$, with a limiting strain $\varepsilon_u=0.003$ and stress $0.72f'_c$, at which crushing is assumed to take place. The stress-strain diagram of the reinforcing steel was assumed elastoplastic.

3.2 Results of Analysis: The ultimate interaction diagram N vs. M for the section is shown in Fig. 6. The inside curves show the variation of the total moment M + ΔM, with N for various values of the ratio e/t ranging from -0.5 to 1.0. Two sets of curves are shown; one corresponding to positive, the other to negative values of e/t and ΔT. Both sets of curves have common origins at N=0 and terminate at their intersection with the interaction diagram. The example given in Table 1 is solved in Fig. 6 for ΔT=100°F. The result of the inelastic analysis for ΔT=50°F shows ΔM=1367 k-in. vs. 1335 k-in. given by the elastic analysis, see Table 1. The larger value given by the inelastic analysis may be attributed to the greater slopes, i.e. tangent modulus, of the concrete stress-strain diagram at lower stresses as compared to the secant modulus used in the elastic analysis. A comparison of results of elastic vs. inelastic analysis when ΔT=100° is given in Fig. 7 for three values of e/t. It is easily seen that, for lower values of N, the inelastic analysis gives larger values of ΔM; the reverse is true as the load N is increased. This is due to the softening of the section as the steel reinforcing yields and the concrete stresses increase to a level where the tangent modulus is small, or even negative as in the descending portion of the curve [7]. The inelastic analysis takes into account these conditions; it is more realistic always, but especially so for advanced loading.

The direct variation of the induced thermal moment ΔM with N, for various eccentricity ratios ranging from -0.5 to 1.0, is shown in Fig. 8. It can be seen that for any value of e/t there is a maximum ΔM created by a certain N beyond which, the induced thermal moment is reduced rapidly as the value of N increases. For any given value of N, the maximum ΔM is obtained with the smallest eccentricity ratio; a logical conclusion, considering the fact that the extent of cracking and consequent loss of stiffness in the section due to thermal effects are smaller as the eccentricity ratio decreases.

In view of the fact that thermal effects do not induce additional axial loads in wall sections of unattached containments, a simple graphical solution of the problem can be obtained with a set of M-ϕ curves drawn for constant N. This is shown in Fig. 9(b) for various values of the ratio N/N_u, where N_u is defined as the maximum load taken by the section when ϕ=0 and ε_c=0.002, see Fig. 6. The induced thermal moment can be readily obtained for any given value of M and N/N_u using Fig. 9(b). Upon location of the point with the given M on the corresponding N/N_u curve, one need only add graphically to its abscissae the value $\phi_T=\alpha\Delta T$, after which proceeding vertically to intersect the curve yields ΔM. Obviously, the effect of negative ϕ_T may be obtained similarly by subtracting from the given abscissae. Since the slope of the various curves is different, it is easy to see from Fig. 9(b) that for any given M, the induced moment ΔM depends on the value of N/N_u. As the slope diminishes for the higher values of M, thermal curvatures induce smaller moments. Significantly, for N/N_u=0, any thermal effect in the flat portion of the curve results in a very small ΔM.

The variation of ΔM with M for various values of N/N_u is given in Fig. 9(a). The largest effects occur when N/N_u is close to 0.4. This value corresponds closely to that of N_B, the load at the balanced point, see Fig. 6; a condition that exists in a section when, at failure, the tension steel is at initial yielding. It is likely that for any given section maximum thermal effects occur when subjected to axial loads close to the balanced load.

4. CONCLUSIONS

As a result of the preceding work, the following conclusions are drawn:

1. For a given section, the moment induced by a given thermal differential depends on the external axial load and bending moment to which the section is subjected.
2. Upper and lower limits exist for elastically determined thermal moments in any section under a given thermal differential. The upper limit is given by the product of the modulus of elasticity of concrete, the thermal curvature and the moment of inertia of the uncracked section. The lower limit is given by a similar product, except that the moment of inertia of the cracked section is used.
3. At service load conditions, elastic analysis renders thermal effects that are smaller than those obtained using inelastic analysis. The reverse is true for higher levels of loading.
4. Inelastic analysis should be used to determine thermal effects in walls of containment structures. Ultimate conditions, and hence, safety of design, can only be determined using inelastic analysis.

5. ACKNOWLEDGMENTS

This investigation was proposed and sponsored by Sargent & Lundy Engineers of Chicago, Illinois and the Civil Engineering Department of the University of Illinois at Urbana. The elastic analysis was carried out by the writer during the summer of 1970 for Sargent & Lundy's Analytical & Computer Division. The inelastic analysis was accomplished at the University of Illinois during the fall semester of this academic year. The author is grateful to M. Zar, S. L. Chu, A. Walser and J. Kontoudakis, of Sargent & Lundy, and R. Wetzel of the University of Illinois, for assistance rendered during the investigation.

REFERENCES

[1] ACI Standard 318-63, "Building Code Requirements for Reinforced Concrete," American Concrete Institute, P. O. Box 4754 Redford Station, Detroit, Mich. 48219.

[2] ACI Special Publication No. 3, "Reinforced Concrete Design Handbook - Working Stress Design," 3rd Edition.

[3] ACI Special Publication No. 7, "Ultimate Strength Design of Reinforced Concrete Columns."

[4] KHACHATURIAN, N., GURFINKEL, G., "Prestressed Concrete," Chapter 11, McGraw-Hill Book Company, N. Y., 1969.

[5] TAN, C. P., "Concrete Containment for Reactors - State of Art," Journal of the Structural Division, ASCE, Vol. 96, No. ST7, Proc. Paper 7424, July 1970, pp. 1543-1566.

[6] GURFINKEL, G., "Thermal Effects in Walls of Nuclear Containments," Internal Report No. 42 of the Analytical and Computer Division of Sargent & Lundy Engineers, Chicago, Illinois, August 1970.

[7] HOGNESTAD, E., "A Study of Combined Bending and Axial Load in Reinforced Concrete Members," Bulletin No. 399, University of Illinois Engineering Experiment Station, Urbana, 1951.

[8] TODESCHINI, C. E., BIANCHINI, A. C., and KESLER, C. E., "Behavior of Concrete Columns Reinforced with High-Strength Steels," Journal of the American Concrete Institute, Vol. 61, No. 6, June 1964, pp. 701-716.

[9] KUPFER, H., HILSDORF, H. K., and RUSCH, H., "Behavior of Concrete Under Biaxial Stresses," Journal of the American Concrete Institute, Vol. 66, No. 8, August 1969, pp. 656-666.

[10] GURFINKEL, G., and ROBINSON, A. R., "Determination of Strain Distribution and Curvature in a Reinforced Concrete Section Subjected to Bending Moment and Longitudinal Load," Journal of the American Concrete Institute, Vol. 64, No. 7, July 1967, pp. 398-403.

Table 1. Illustration of Iteration Method*

CYCLE	a (in)	$N(e'+a)$ Kip-in	$E\bar{I}\phi_t$ Kip-in	$-NI/S$ Kip-in	R Kip-in
1	24.00	2612.41	776.91	- 6226.78	- 2837.46
2	11.82	-1039.75	646.33	-47225.92	-47619.34
3	24.77	2843.82	798.53	- 6221.82	- 2579.47
4	25.51	3066.25	821.21	- 6236.44	- 2348.98
5	33.06	5333.12	1176.19	- 7005.70	- 496.39
6	35.09	5940.51	1314.42	- 7315.91	- 60.98
7	35.38	6025.58	1335.39	- 7361.30	- 0.33

* For the given case: b=12 in, t=48 in, A_s=2.75 in^2, d=45 in, A_s=1.25 in^2, d'=10 in, f'_c=4.5 ksi, E=3865 ksi, f_y=60 ksi, E_s=29,000 ksi, n=7.5, T_1=110°F, T_2=60°F, ΔT=50°F, α=5.5x10^{-6}/°F, ϕ_T=5.72x10^{-6} in^{-1}, N=300 kips, M=2880k-in, e=9.6 in, e'=-15.29 in; $\bar{I}$, I, S and R depend on the value of a. The thermal moment ΔM=1335 k-in.

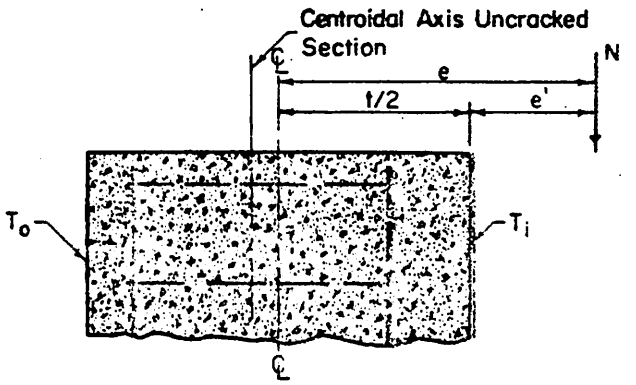

(a) Vertical Section of Wall

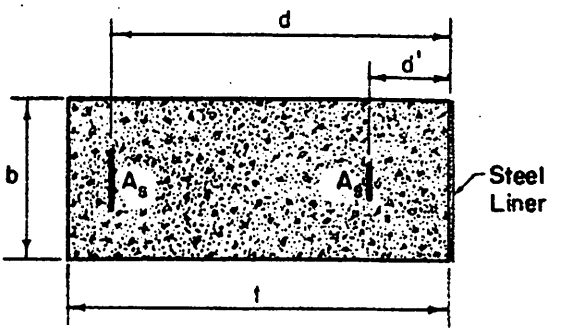

(b) Horizontal Section of Wall

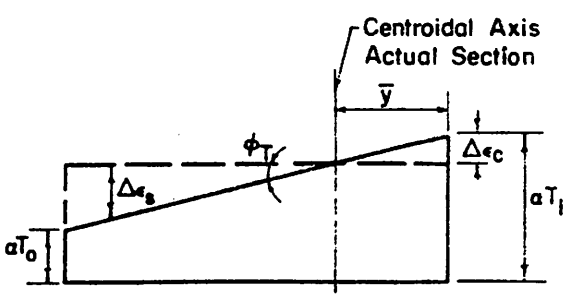

(c) Temperature Strains

FIG. 1 CONTAINMENT WALL UNDER ECCENTRIC LOADING AND THERMAL DIFFERENTIAL

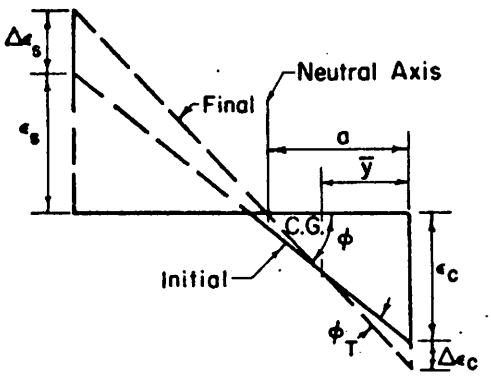

(a) Strain Distribution

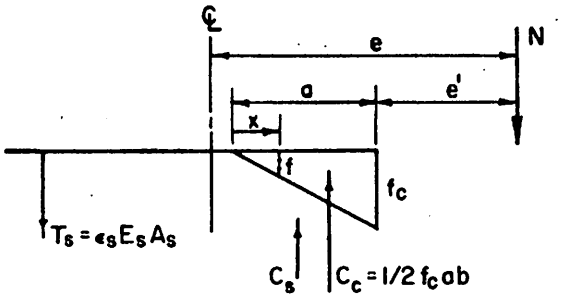

(b) Stress Distribution, Elastic

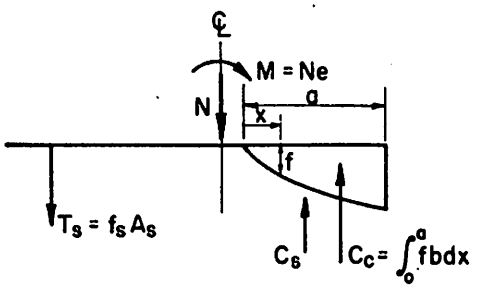

(c) Stress Distribution, Inelastic

FIG. 2 STRAIN AND STRESS DISTRIBUTIONS IN CONTAINMENT WALL

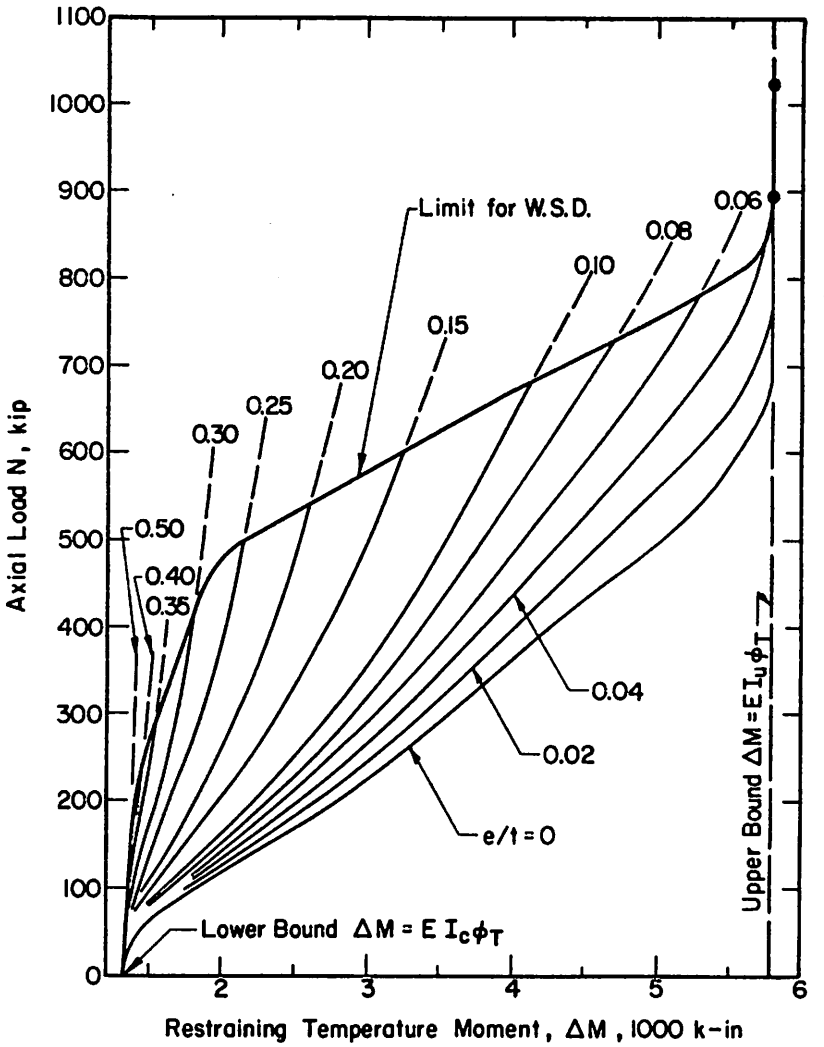

FIG. 3 THERMAL MOMENTS IN A GIVEN SECTION UNDER 100° F TEMPERATURE DIFFERENTIAL. ELASTIC ANALYSIS

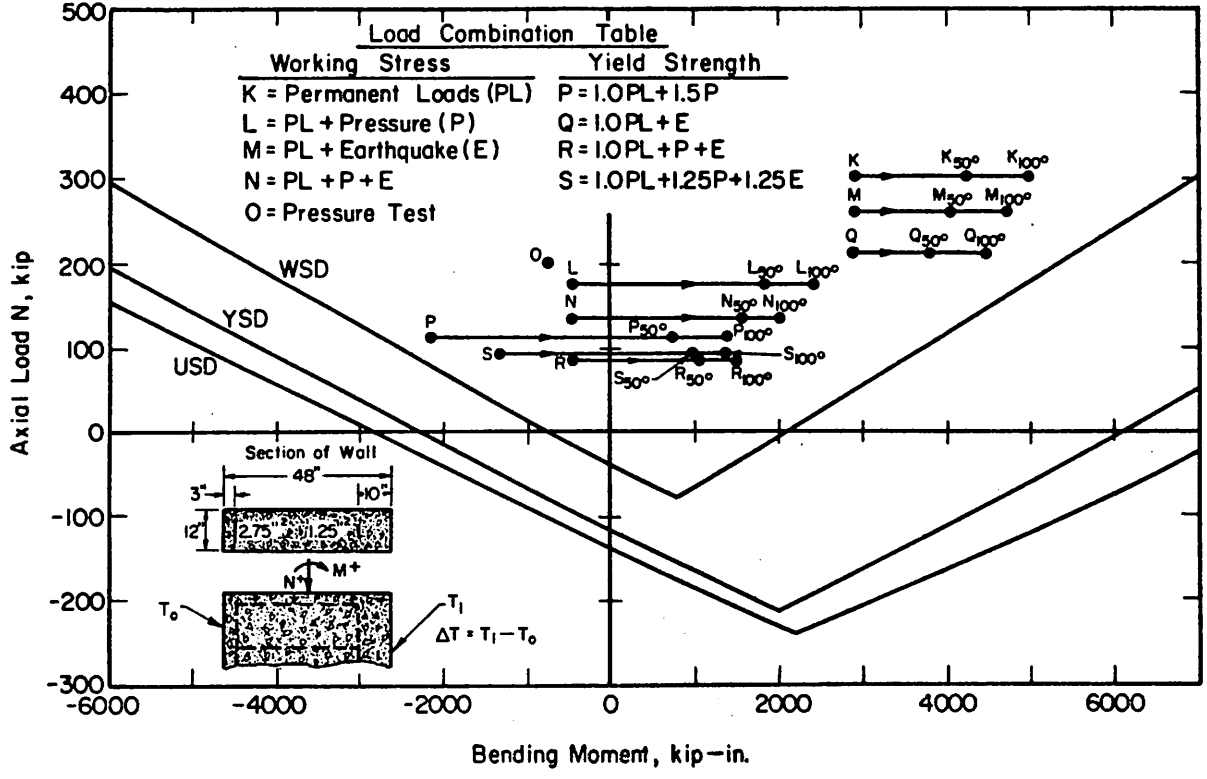

FIG. 4 THERMAL EFFECTS IN WALL OF ACTUAL CONTAINMENT

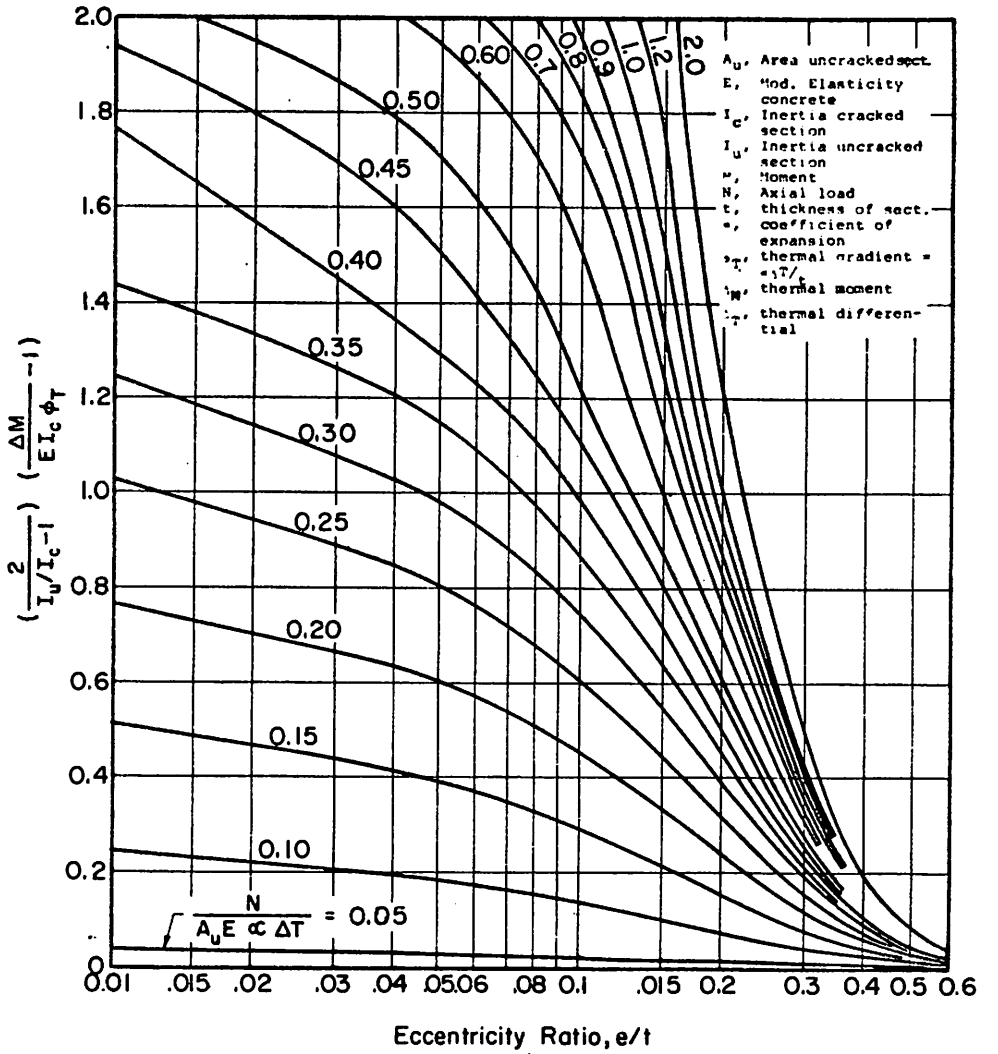

FIG. 5 APPROXIMATE DETERMINATION OF THERMAL EFFECTS FOR ANY GIVEN SECTION. ELASTIC ANALYSIS

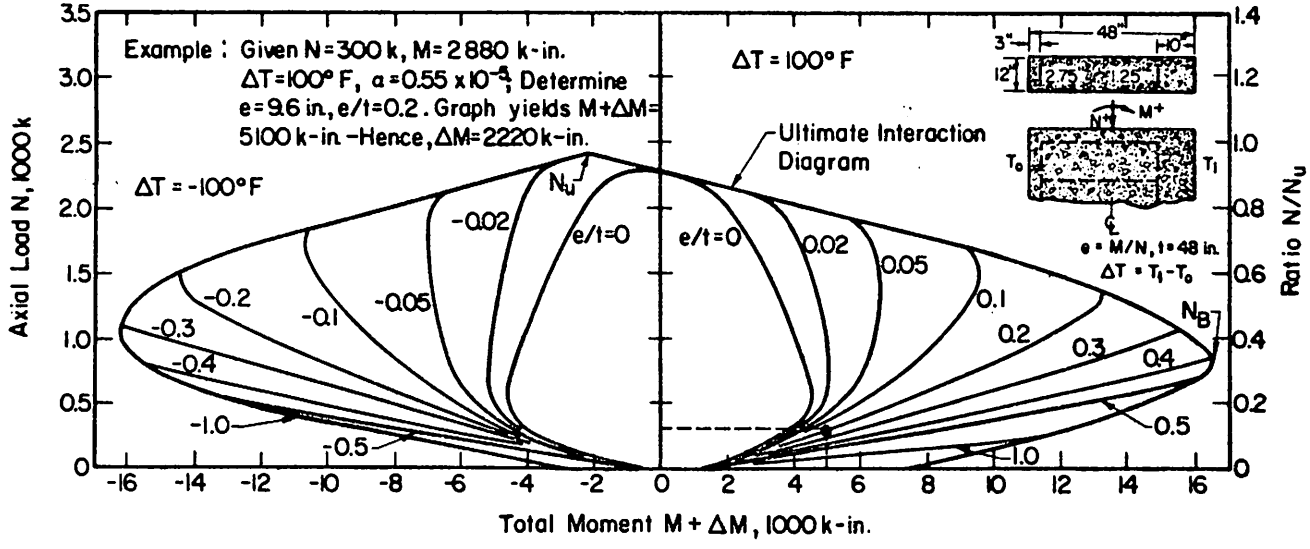

FIG. 6 THERMAL EFFECTS IN A GIVEN SECTION FOR VARIOUS ECCENTRICITY RATIOS. INELASTIC ANALYSIS

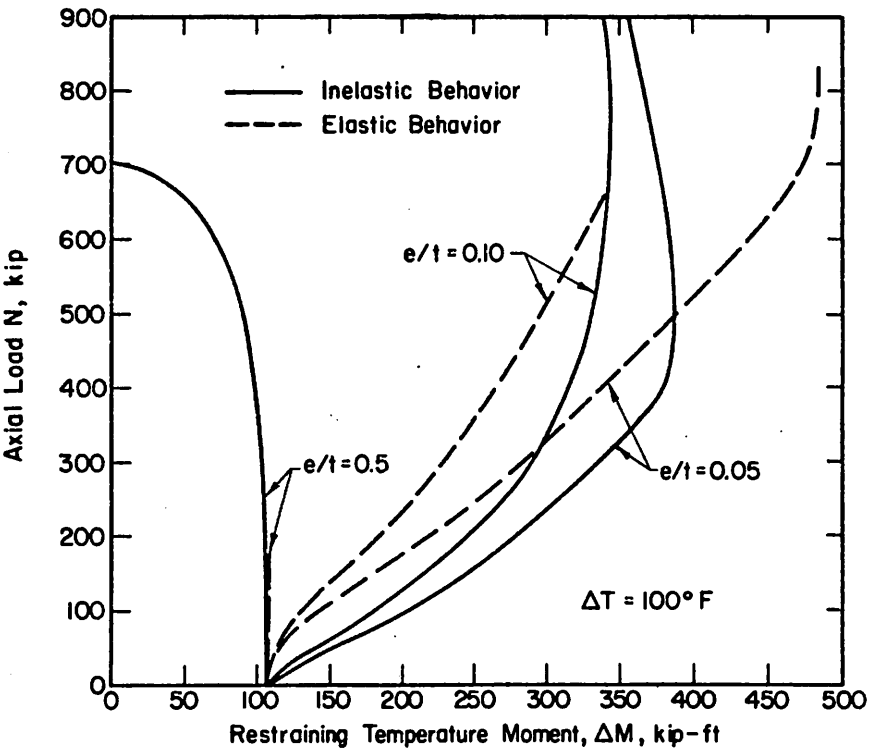

FIG. 7 COMPARISON OF ELASTIC VS. INELASTIC THERMAL EFFECTS

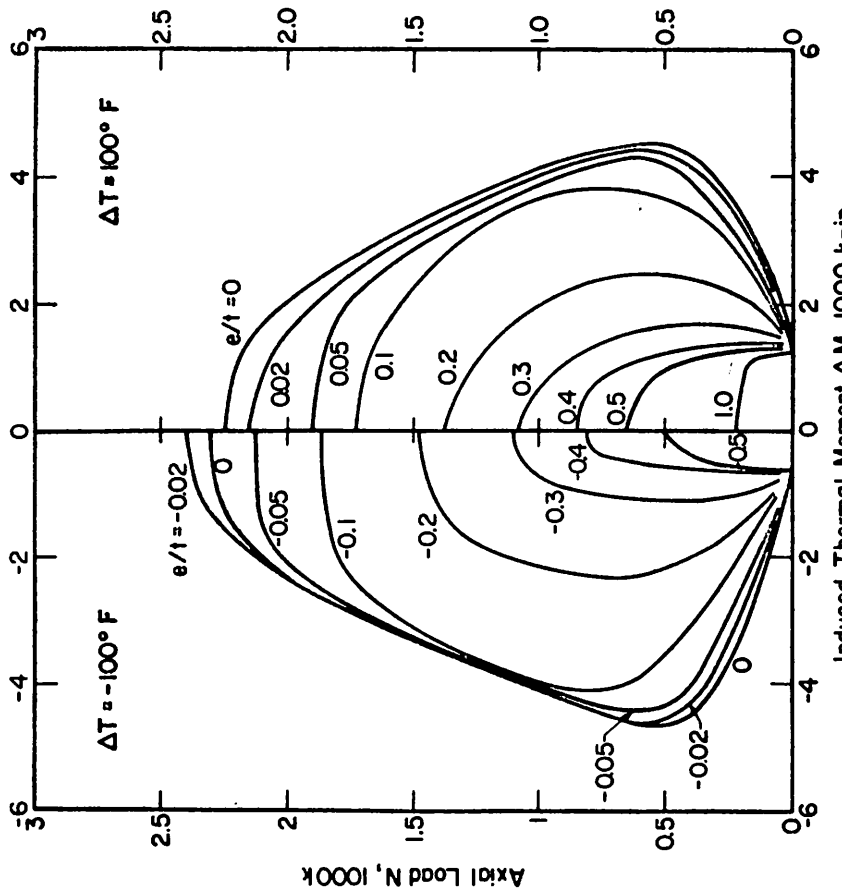

FIG. 8 THERMAL EFFECTS IN A GIVEN SECTION UNDER 100° F TEMPERATURE DIFFERENTIAL. INELASTIC ANALYSIS

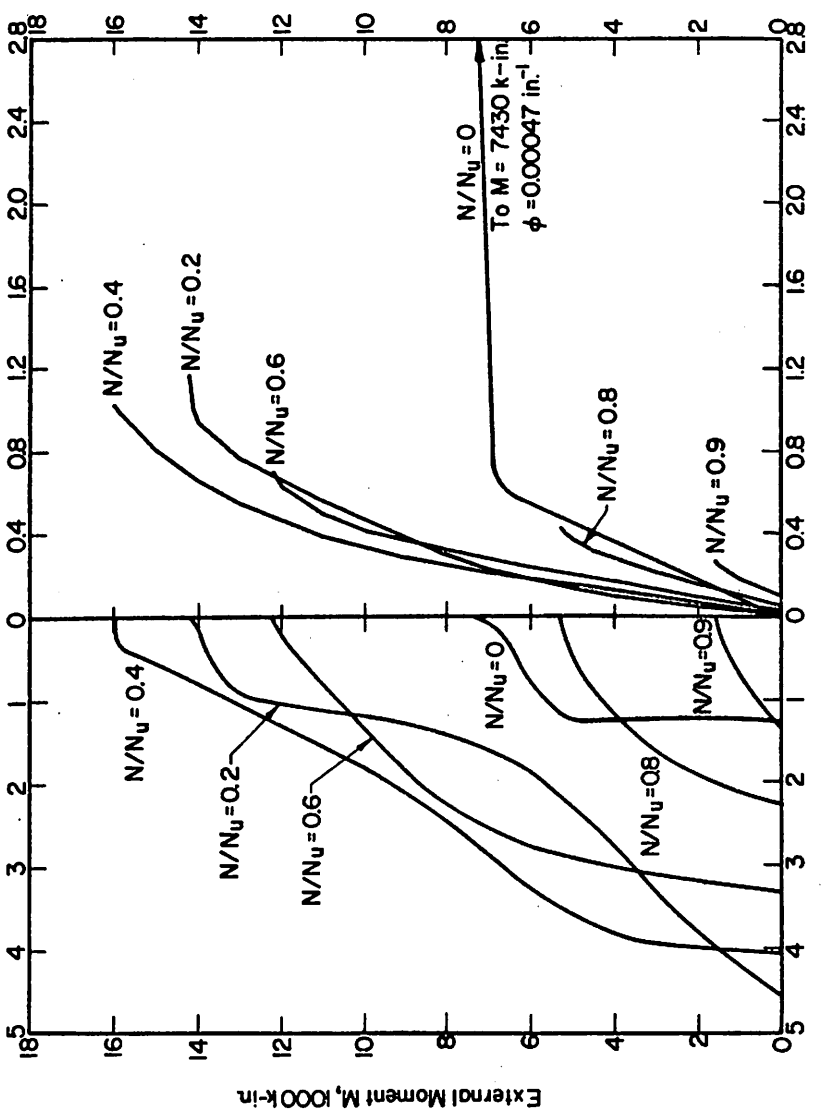

FIG. 9 THERMAL EFFECTS AND MOMENT-CURVATURE RELATIONS IN A GIVEN SECTION FOR VARIOUS AXIAL-LOAD RATIOS

DISCUSSION

Q R. S. BEKOWICH, U. S. A.

1. Does the method discussed apply to the analysis of the containment around a large opening such as an equipment notch ?

2. Does the method take into consideration the various materials present such as concrete reinforcing steel, liner, and prestressing. Also does it consider the effect of concrete cracking ?

A J. M. DOYLE, U. S. A., p. p. G. GURFINKEL, U. S. A.

1. The methods presented in the paper were applied only to areas of the containment located away from any openings or penetrations. That is, in a section with no discontinuities in geometry.

2. The analysis included the effects of reinforcing steel and cracking of the concrete. It did not include the effect of the liner.